Task allocation and planning for product disassembly with human–robot collaboration

Article *in* Robotics and Computer-Integrated Manufacturing · August 2022

DOI: 10.1016/j.rcim.2021.102306

CITATIONS
6

READS
286

4 authors:

Meng-Lun Lee
University at Buffalo, The State University of New York
5 PUBLICATIONS **14** CITATIONS
SEE PROFILE

Sara Behdad
University of Florida
113 PUBLICATIONS **2,142** CITATIONS
SEE PROFILE

Xiao Liang
University at Buffalo, The State University of New York
66 PUBLICATIONS **664** CITATIONS
SEE PROFILE

Minghui Zheng
University at Buffalo, The State University of New York
74 PUBLICATIONS **589** CITATIONS
SEE PROFILE

Robotics and Computer–Integrated Manufacturing 76 (2022) 102306

Contents lists available at ScienceDirect

Robotics and Computer-Integrated Manufacturing

journal homepage: www.elsevier.com/locate/rcm

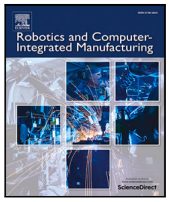

Full length article

Task allocation and planning for product disassembly with human–robot collaboration

Meng-Lun Lee [a], Sara Behdad [b], Xiao Liang [c,*], Minghui Zheng [a,*]

[a] Department of Mechanical and Aerospace Engineering, University at Buffalo, Buffalo, NY 14260, USA
[b] Department of Environmental Engineering Sciences, University of Florida, Gainesville, FL 32611, USA
[c] Department of Civil, Structural and Environmental Engineering, University at Buffalo, Buffalo, NY 14260, USA

ARTICLE INFO

Keywords:
Human–robot collaboration
Task planning

ABSTRACT

This paper presents a comprehensive disassembly sequence planning (DSP) algorithm in the human–robot collaboration (HRC) setting with consideration of several important factors including limited resources and human workers' safety. The proposed DSP algorithm is capable of planning and distributing disassembly tasks among the human operator, the robot, and HRC, aiming to minimize the total disassembly time without violating resources and safety constraints. Regarding the resource constraints, we consider one human operator and one robot, and a limited quantity of disassembly tools. Regarding the safety constraints, we consider avoiding potential human injuries from to-be-disassembled components and possible collisions between the human operator and the robot due to the short distance between disassembly tasks. In addition, the transitions for tool changing, the moving between disassembly modules, and the precedence constraint of components to be disassembled are also considered and formulated as constraints in the problem formulation. Both numerical and experimental studies on the disassembly of a used hard disk drive (HDD) have been conducted to validate the proposed algorithm.

1. Introduction

The growing amount of electronic waste (e-waste) has been receiving increasing attention in the recycling industry [1–3]. The e-waste disassembly process is usually time-consuming and labor-intensive [4–7]. The disassembly sequence should not be considered as the reverse of the assembly [8–10], since the components to be disassembled may have different conditions, such as missing parts, corrosion, or other hazardous substances and attributes that need to be handled cautiously. In addition, a typical assembly line is usually conducted in a work-cell format with serial workstations, customized fixtures [11] and robots that are programmed for repetitive tasks [12,13], while the disassembly process for the distinctive e-waste may be loaded to the same disassembly line in the recycling facility with various conditions and arbitrary orientations. Thus, the conduct of the sequence planning for the use of robots in disassembly settings is more challenging than that in assembly settings and needs further investigation.

There has been an increasing amount of used high-precision electronics and products such as hard disk drives, cell phones, and computers. Many factors, including environmental sustainability and potential profitability of recycling and reusing costly materials, have driven us to consider recycling these used products. Disassembly is the first and the most critical step in the remanufacturing process [14,15]. The to-be-disassembled products possess many attributes that do not appear in the assembly line, such as the same component with different conditions, multiple choices for the same disassembly task, and even different brands of products in the same disassembly line. Furthermore, the information of the to-be-disassembled component may be missing or incorrect, causing the difficulty of obtaining the optimal disassembly sequence. Needless to say, the decisions of assigning workers to the disassembly tasks become more complex while both humans and robots are available [16]. A comprehensive review on human–robot collaborative disassembly is provided in [17].

Task sequence planning plays an important role to reduce the disassembly cost such as time. There exist several methods to model the planning problem and obtain the disassembly sequence. One commonly used approach is to explore potential sequences indicated by graph visualization [18]. The graph-based representation is usually obtained via a computer-aided design (CAD) database [19] or from the physical information generated by the user. For instance, the CAD data is used with visual data in [20] to conduct a disassembly sequence for a pneumatic valve. A cognitive robotic-based system, capable of reasoning, execution monitoring, learning and revision for the disassembly, is

* Corresponding authors.
E-mail addresses: menglunl@buffalo.edu (M.-L. Lee), sarabehdad@ufl.edu (S. Behdad), liangx@buffalo.edu (X. Liang), mhzheng@buffalo.edu (M. Zheng).

https://doi.org/10.1016/j.rcim.2021.102306
Received 23 June 2021; Received in revised form 14 December 2021; Accepted 16 December 2021

investigated extensively in [21], which shows that the vision-based disassembly system is able to adjust to any product model without prior information. In addition, a system for the electric motor disassembly is investigated in [22], in which the screws are detected based on their characteristics concerning the gray-scale, depth and RGB (Red–Green–Blue) color model. Thus the disassembly does not need to perform template matching with an image database. A hybrid metaheuristic algorithm is proposed in [23] for a profit-oriented and energy-efficient disassembly sequencing planning, in which it is formulated into an multi-objective optimization problem.

In fact, the graph-based modeling can be represented in several forms to find disassembly planning sequences for robotics, such as AND/OR graphs [24,25], directed graphs [26], precedence diagrams [27,28], and Petri-net [29]. In addition, optimization problems have been investigated to obtain the disassembly sequence. For example, [30,31] formulate the sequence planning problem into a traveling salesman problem. The scheduling problems, including the multi-mode resource-constrained project scheduling problem [32] and flexible job-shop scheduling problem [33,34], are also investigated such that the tasks can be assigned with limited resources at particular times. However, most of these methods have not considered any robotic incorporation.

Disassembly sequence planning is proven to be an NP-hard problem because of multiple constraints in calculating optimality [35–38]. As the quantity of the e-waste components increases, the search space for feasible solutions grows rapidly [39]. There are several recently-developed algorithms to obtain the optimal or a sub-optimal sequence efficiently. Most of the searching algorithms belong to the heuristic approach [24,40]. One commonly used algorithm is the generic algorithm. For example, a genetic algorithm-based optimization approach is proposed in [41] to determine the disassembly sequence. An automotive component remanufacturing through the end-of-life stage of mechanical products using the genetic algorithm is studied to solve the fitness function, which is dependent on the change in the disassembly time [42]. Optimal or near-optimal solutions have been obtained by the genetic algorithm in [43] for solving the disassembly line balancing problem (DLBP) [2,44,45], which is defined as assigning disassembly tasks to workstations such that all precedence relationships between tasks are satisfied and some measures of effectiveness are optimized. There are also other algorithms such as ant colony optimization, particle swarm optimization and artificial bee colony algorithm. For example, [46] uses ant colony optimization and considers component numbers, disassembly tools and disassembly directions in the disassembly sequence planning problem. [47] uses an ant colony optimization algorithm to solve the multi-objective disassembly line balancing problem. [48] proposes an approach based on particle swarm optimization with a neighborhood-based mutation operator to solve the sequence-dependent disassembly line balancing problem. In addition, the artificial bee colony algorithm is used to make decisions regarding energy savings for the disassembly line balancing problem [49], and its fuzzy extension, the hybrid discrete artificial bee colony algorithm, is proposed to deal with the uncertainty of the real-world disassembly systems [50]. Additionally, failed disassembly operations are formulated as unpredictable factors in a profit-based disassembly sequence planning in [51]. The other methods, such as artificial neural network and artificial intelligence techniques, are commonly applied to solve the DSP problem [52,53]. However, these methods demand high computational effort. A study in [54] presented a robotic disassembly system that aims to solve some challenges in real applications. Nevertheless, the current disassembly process is still labor-intensive and usually accomplished manually.

To facilitate the disassembly process, human–robot collaboration (HRC) has been introduced to exploit the complementary advantages of humans and robots, as humans have experience and demonstrate better reactions to uncertainties in assignments. In contrast, robots provide accuracy and handle unsafe tasks that could cause human injuries. From the perspective of production planning, which plans and allocates

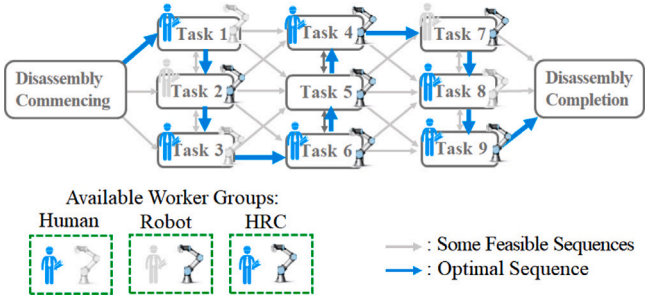

Fig. 1. Example of task planning with 9 tasks.

components, workers, and workstations to fulfill task orders on time, the utilization of robots in their collaboration with human workers is promising to increase production efficiency while poses new challenges to the traditional scheduling problems. For example, decisions have to be made regarding which tasks should be executed by a human operator and which tasks be left to the robot. In addition to finding the time-efficient disassembly sequence, [55] proposes a method that aims to minimize the total disassembly time for the human–robot collaboration with the consideration of human fatigue, which occurs more frequently in the same type of disassembling process. A human–robot collaborative disassembly line balance problem (HRC-DLBP) is proposed in [56] to improve the efficiency of disassembly and reduce the disassembly cost, which considers the energy consumption and disassembly failure using multi-objective artificial bee colony algorithm (MOABC) [57,58]. A multi-product partial disassembly line balancing problem with multi-robot workstations (MPR-PDLBP) is proposed in [59], which establishes a mixed-integer programming (MIP) model to find the solutions of optimization objectives, including hazardous index, cycle time and energy consumption. Furthermore, a discrete artificial bee colony algorithm is applied to a liquid-crystal display (LCD) television disassembly with multiple disassembly schemes to minimize the makespan and energy consumption [60]. A computer case disassembly is studied to develop HRC planning using a modified discrete bees algorithm based on Pareto (MDBA-Pareto) [61,62], a multi-objective optimization method aiming to minimize the disassembly time, disassembly cost and disassembly difficulty. Besides the challenges in scheduling when introducing human–robot collaboration in disassembly, other challenges such as communication among human and robot operators exist as well, which are traditionally difficult in both assembly [63] and disassembly. Nevertheless, though introducing HRC to disassembly is promising to facilitate the disassembly process and reduce the labor cost, the above-mentioned challenges are very difficult to overcome.

In addition, the temporal and spatial safety distances between robots and human operators need to be considered and assured during the task allocation and sequence planning. There have been many applications and studies (e.g., elderly care [64], space applications [65], rescue robotics [66], and assembly lines [67,68]) on task allocation and planning considering HRC. For example, a recent experimental study [69] on HRC considers human situational awareness, workload allocation and human workflow preferences, and the underlying formal scheduling problem is formulated as a time-indexed integer linear programming (ILP) model. Another example is the deployment of a multi-robot system in a warehouse [70], in which the robots move merchandise and equipment from one place to another in collaboration with human operators. However, those studies are not particularly focusing on the complex disassembly sequence planning problem and do not consider the transition time caused by tool changing and traveling between different disassembly modules.

Fig. 1 shows an example of human–robot collaboration, in which the gray arrows indicate the possible task sequence and the blue arrows

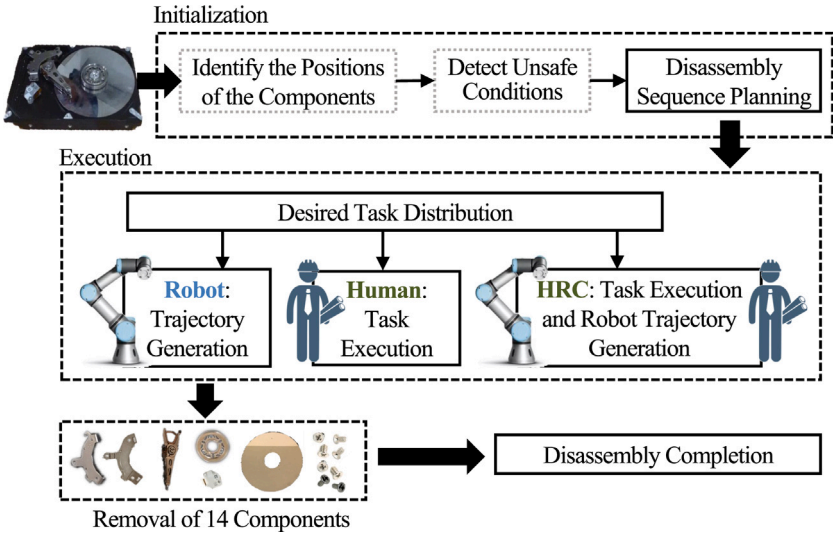

Fig. 2. Proposed framework of DSP.

indicate the optimal task sequence. During the searching of the optimal sequence, many practical factors regarding disassembly efficiency, human worker's safety, limited tools and resources, etc., need to be considered, which makes the sequence planning problem very complex.

There have been limited research that is particularly on human–robot collaborative disassembly. In [71], human behavior is recognized via deep learning techniques during the decision making process. In [72], the sequence planning considering HRC is handled via a hybrid resource assignment and scheduling problem via mixed-integer linear programming. In [73], a robotic disassembly cell with two collaborative robots and a human operator using force and positional control is presented to conduct the disassembly tasks. [74] presents a disassembly planning method in the human–robot setting for end-of-life product while considering three remanufacturability factors: cleanability, reparability, and economy. In our previous work [75,76], the safe condition is introduced when planning the disassembly sequence in the HRC setting. However, most of the above-mentioned studies on HRC for disassembly do not provide a comprehensive HRC framework and many important factors/constraints such as the human workers' safety are not explicitly considered.

We propose a comprehensive sequence planning algorithm in the HRC setting with explicitly considering multiple factors as listed in the following.

- *Transition time realization*: The transition occurs when workers need to (1) receive/return the tool or (2) move from a disassemble module to another disassemble module. To eliminate the unnecessary transitions in the disassembly, the proposed sequence planner is capable of assigning a worker to finish a series of tasks that require the same tool, or tasks that belong to the same disassembly module. More details will be explained in the problem formulation section.
- *Resource constraints*: In the real-world scenario, the numbers of human operators, robots and disassembly tools are strictly limited. Hence, in this paper we limit the available number of human operators and robots at each instant as well as the number of tools required for the disassembly tasks.
- *Disassembly rules*: Similar to an assembly, components in the disassembly product must be removed following strict orders. The precedence constraints of the disassembly cannot be violated due to the nature of the hardware design.
- *Cost of operations by robot and human operator*: The disassembly tasks can be performed in parallel or in serial by the human operator, the robot, or both the human operator and the robot. To find the optimal sequence of disassembly, the cost of each disassembly action needs to be quantified. In this paper, we parameterize the cost as the combination of the travel distances between the to-be-disassembled components and the robot/human operator, and the time spent on the tasks.
- *Safety of human operator*: It is assumed that handling hazardous materials and other situations of hazards [77] may occur during the disassembly sequence. Hence, the possible cases of dangerous human actions and human–robot interactions should be detected before assigning disassembly tasks. To avoid potential human injuries, the task planner must assign the robot to disassemble the component instead of the human operator. Thus, safety requirements should be considered regardless of the disassembly cost using a robot. Also, some tasks are too close to be done by both the human worker and the robot in parallel and minimum safety distance has to be guaranteed at the sequence planning level.

The main contribution of this paper is that we propose a comprehensive sequence planning algorithm among human, robot, and human–robot collaboration with explicitly considering multiple practical constraints, including transition time, resource constraints, disassembly rules, and safety of human workers, and mathematically formulate them into an optimization problem. The formulation itself is complex and challenging. Compared to existing disassembly sequence planning using human–robot collaboration, the highlights of our formulation are listed as follows. (1) Most of the literature only considers human and robot, as two work groups, in the sequence planning; our work considers human, robot, and human–robot collaboration, as three work groups. That is to say, the tasks have been classified into three categories: the ones for robot, the ones for human, and the ones for human–robot collaboration; while in most literature the tasks have been classified into two categories: the ones for robot and the ones for human. The tasks that can be done via human–robot collaboration are not particularly considered separately. (2) Most of the literature on human–robot collaborative disassembly sequence planning does not consider the time spent on either tool-change or the transition between different disassembly modules. (3) Most of the literature considers human safety at the motion planning level instead of the task sequence planning level.

It is noted that the proposed task planning algorithm may be used to disassemble hard disk drives (or other electronic wastes) and incorporate the following scenarios: (1) the application has multiple tasks with different tools requirements, (2) the application has limited quantity of tools, (3) the application has multiple modules that consist

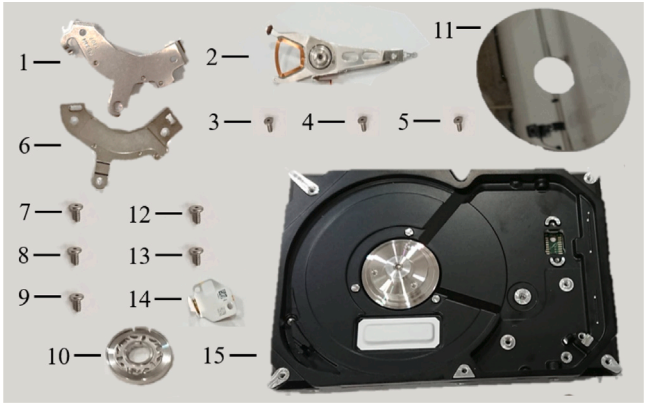

Fig. 3. Disassembled components of a used HDD.

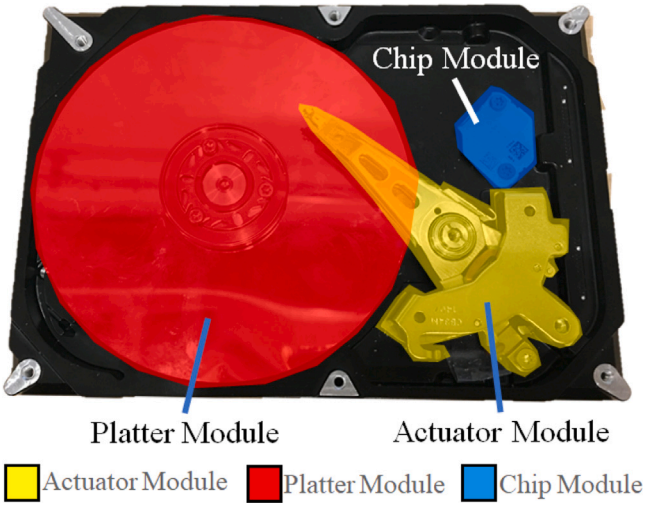

Fig. 4. Three modules on a Used HDD (Referring to Table 2). (For interpretation of the references to color in this figure legend, the reader is referred to the web version of this article.)

of many tasks, (4) the application has multiple workers capable of performing the same task(s), and (5) the application may have tasks that are unsafe for human operation. Also, it is worth mentioning that the precedence graph is not enough for an expert to automatically derive the plan. The reason is that the precedence graph only shows possible disassembly orders of the components. Due to the human–robot collaboration setting as well as many other constraints such as safety and limited resources, the disassembly sequence cannot be simply obtained from the precedence graph.

The remainder of this paper is structured as follows: Section 2 introduces the problem formulation, including the assumptions, parameters and decision variables, performance index and the constraints. Section 3 presents numerical studies of the hard disk drive (HDD) disassembly with two simulated scenarios. Section 4 provides experimental studies to validate the proposed disassembly planning. Section 5 concludes the paper.

2. Assumptions and problem formulation

In this section, we introduce the disassembly sequence planner in detail. Assume there are n components to be disassembled and each component corresponds to a disassembly task. The tasks can be assigned to one of the worker groups: the human operator, the robot, or the human operator and the robot together (HRC mode). Each disassembly task j is specified by its processing time p_{jw} with the corresponding worker group w. In this paper, the goal is to remove components 1 to 14 from Component 15 (HDD base), as listed in Fig. 3. The reproduction value and the energy consumption of the disassembled component are beyond the scope of the paper. Although it is possible to only disassemble certain components, in this paper we endeavor to demonstrate and solve the disassembly sequence planning with sufficiently large number of disassembly tasks in a human–robot collaboration setting.

Next, we assume that the CAD file of the HDD is absent, so the positions of the HDD components, precedence relationships between the components, and the grasp poses and the required disassembly tools for each component are defined by human preliminarily. Additionally, each disassembly task can be assigned to one of the three worker groups. Unsafe tasks will be assigned to the robot to prevent human injury. When the task is assigned, the agents will not work on the other task until the assigned task is complete. The disassembly tasks have sets of succeeding tasks and can be performed by a human operator, a robot, or HRC with different processing periods. When a task is assigned to HRC consisting of a human operator and a robot, both the human operator and the robot will be acquired for the same disassembly task. We also assume that the human operator and the robot perceive their roles in a task assigned to HRC. In addition, disassembly tasks may require certain disassembly tools and the quantity of each tool is limited to one. When a scheduled task requires a specific tool, another task requiring the same tool cannot be performed at the same time. With these reasonable assumptions, the proposed sequence planner aims to find the optimal scheduling for a set of n tasks subject to constraints, which includes: (1) task assignment with the three worker groups (human operator, robot, and HRC), (2) unsafe task allocation, (3) non-preemptive task scheduling, (4) precedence relationships, (5) number of the human operator and the robot, (6) safety distance between the human operator and the robot in disassembly tasks, (7) tool availability, (8) tool-changing time, and (9) transition penalty between disassembly modules. Each constraint will be briefly explained below. The flow chart of the proposed task planning is shown in Fig. 2.

We will first introduce the notations of the problem formulation for the HDD disassembly. An instance of the HDD disassembly comprises the parameters and decision variables, which are listed in Table 1. The decision variable x_{jwt} determines whether Task j will be assigned to the worker group w (the human operator, the robot, or HRC) at time t. The mathematical formulation for the HDD disassembly problem is shown below.

Optimization problem:

$$\min_{x_{jwt}} \sum_{t\in T}\sum_{w\in W} t \cdot x_{n+1,w,t} \tag{1}$$

Subject to

$$\sum_{t\in T}\sum_{w\in W} x_{jwt} = 1 \tag{2}$$

$$\sum_{t\in T}\sum_{w\in W} x_{jwt} = 0 \quad j \in J_u, w \neq \text{Robot} \tag{3}$$

$$\sum_{t\in T} x_{jwt} = 1 \quad j \in J_u, w = \text{Robot} \tag{4}$$

$$\sum_{j\in J}\sum_{k=t-p_{jw}+1}^{t} x_{jwk} \leq 1 \quad \forall w \in W, \quad t \in T \tag{5}$$

$$\sum_{w_2\in W}\sum_{t_2\in T} t_2 \cdot x_{jw_2t_2} - \sum_{w_1\in W}\sum_{t_1\in T}(t_1 + p_{iw_1}) \cdot x_{iw_1t_1}$$

$$\geq 0, \quad (i,j) \in S \tag{6}$$

$$\sum_{j\in J}\sum_{w\in W}\sum_{k=t-p_{jw}+1}^{t} c_{jw} \cdot x_{jwk} \leq 2 \quad \forall t \in T \tag{7}$$

Table 1
(a) Parameters and (b) Decision variables.

Parameters related to the disassembly scenario	
Symbol	Definition
T	Planning horizon for all disassembly tasks, $T \in \mathbb{Z}^+$.
t	Starting time of a disassembly task, $t \in T$.
J	Set of disassembly tasks.
n	Total number of disassembly tasks.
W	Set of worker groups, W = {Human Operator, Robot, both Human Operator and Robot (HRC)}.
w	A worker group, $w \in W$.
p_{jw}	Processing time of task j by worker group w, $p_{jw} \in \mathbb{Z}^+$.
J_p	Task set that the human operator and the robot can work together or in parallel, $J_p \subseteq J$.
J_u	Task set unsafe for human operation, $J_u \subseteq J$.
S	Set of task pairs with precedence relationships.
M	A sufficiently large number.
D	Set of task pairs that do not meet the minimum safety distance requirement.
I_{ij}	'1' Only if Task i precedes Task j, '0' Otherwise.
c_{jw}	Quantity of worker group w required for Task j.
V	Set of HDD modules. (see Fig. 4)
V_i	Tasks belong to i_{th} HDD module. $V_i \subset V$.
R_b	Maximum quantity of tool b.
r_{jb}	Quantity of tool b required for Task j.
g_w	Transition time spent by worker w.
U	Grouping of tasks requiring specific tools.
U_a	Set of tasks requiring tool a. $U_a \subset U$.
$\bar{U}_a$	Subset of remaining tasks except Task i, $i, \bar{U}_a \in U_a$, $i + \bar{U}_a = U_a$, $i \notin \bar{U}_a$.
(a)	
Decision variables	
Symbol	Definition
x_{jwt}	'1' if Task j assigned to worker group w at time t, '0' Otherwise.
(b)	

$$I_{ij} + I_{ji} = 1 \quad \forall (i,j) \in D \tag{8}$$

$$\sum_{w_1,w_2 \in W} \sum_{t \in T} \left[t \cdot x_{jw_2t} - (t + p_{iw_1}) \cdot x_{iw_1t} \right] \geq M(I_{ij} - 1) \quad ,(i,j) \in D \tag{9}$$

$$\sum_{w_1,w_2 \in W} \sum_{t \in T} \left[t \cdot x_{iw_2t} - (t + p_{jw_1}) \cdot x_{jw_1t} \right] \geq M(I_{ji} - 1) \quad ,(i,j) \in D \tag{10}$$

$$\sum_{j \in J} \sum_{w \in W} \sum_{k=t-p_{jw}+1}^{t} r_{jb} \cdot x_{jwk} \leq R_b \quad \forall t \in T \tag{11}$$

$$\sum_{i \in U_a} \sum_{o=t-p_{jw}-g_w}^{t-1} (o + p_{jw} + g_w) \cdot x_{iwo} \leq \sum_{j \in U_b} t \cdot x_{jwt} + M \cdot \left(1 - \sum_{j \in U_b} x_{jwt}\right)$$

$$\forall t \in T, \quad w \in W, \quad U_a, U_b \subset U, a \neq b \tag{12}$$

$$\sum_{o=t-p_{iw_1}-g_{w_1}}^{t-1} (o + p_{iw_1} + g_{w_1}) \cdot x_{iw_1o} \leq \sum_{j \in \bar{U}_a} t \cdot x_{jw_2t} + M \cdot \left(1 - \sum_{j \in \bar{U}_a} x_{jw_2t}\right)$$

$$\forall t \in T, \quad w_1, w_2 \in W, \quad i, \bar{U}_a \in U_a, \quad i \notin \bar{U}_a \tag{13}$$

$$\sum_{i \in V_a} \sum_{o=t-p_{jw}-g_w}^{t-1} (o + p_{jw} + g_w) \cdot x_{iwo} \leq \sum_{j \in V_b} t \cdot x_{jwt} + M \cdot \left(1 - \sum_{j \in V_b} x_{jwt}\right)$$

$$\forall t \in T, \quad w \in W, \quad V_a, V_b \subset V, a \neq b \tag{14}$$

First of all, Eq. (1) is the performance index that seeks to find the minimum disassembly time. The decision variable $x_{n+1,w,t}$ determines the starting time of Task $(n+1)$, which is a virtual task that serves as the indication of the end of the HDD disassembly. It is worth noting that the processing time for the virtual task is always zero, so when an optimal task sequence is obtained, the task that succeeds Task 0 will be the first task, and the task that precedes Task $(n+1)$ will be the last task in the HDD disassembly.

Constraint (2) ensures that each disassembly task will start at time t and be assigned to one of the three worker groups: the human operator, the robot, or HRC. The decision variable x_{jwt} equals 1 if Task j starts at time t by a worker group w; otherwise, x_{jwt} equals 0. Constraints (3) and (4) together guarantee that unsafe tasks will not be assigned to the human operator to prevent human injuries. The task set J_u in Constraints (3) and (4) contains the unsafe tasks that are detected during the initialization stage (see Fig. 2). The decision variable x_{jwt} in Constraint (3) is set to 0 to prevent the human operator from being assigned to any unsafe tasks in J_u. Similarly, the decision variable x_{jwt} in Constraint (4) becomes 1, forcing the robot to perform the unsafe tasks.

Furthermore, Constraint (5) ensures that, if a worker group w is processing Task j, then Task j will be performed non-preemptively because the worker group w cannot perform two or more tasks simultaneously; in other words, once a worker group w is assigned to a disassembly task j, only one of the decision variables x_{jwt} from t to $t + p_{jw}$ equals 1.

Additionally, the precedence relationships of the to-be disassembled components are conducted in Constraint (6); t_2 and t_1 denote the starting time of Task j and Task i, respectively; and w_2, w_1 indicate the corresponding workers of Task j and Task i, respectively. Since it is a hard constraint inherited by the hardware design, we must guarantee that the disassembly orders of the task pairs in the set S are followed, regardless of the worker group being assigned to the task pair (i,j). For instance, the decision variable $x_{jw_2t_2} = 1$ only appears after passing $t_1 + p_{iw_1}$ seconds with the decision variable $x_{iw_1t_1} = 1$. It is worth noting that the task pairs in S only represent the priorities of the tasks and do not portray the processing of Task j immediately after the completion of Task i.

Because of the limited numbers of the human operator and the robot, optimizing the HDD disassembly can be identified as a resource-constrained scheduling problem with the distribution of the limited quantity of workers as formulated in Constraint (7). The constraint limits at the most only one human operator and one robot can process a task in the time horizon T. For example, if Task j is assigned to the worker group w of HRC (see Task 3 in Figs. 5(a) and 5(c)), the decision variable x_{jwt} will be 1 at time t and none of the other two worker groups can be assigned to any tasks from time t to time $t + p_{jw}$. Moreover, we aim to assign disassembly tasks to the three worker groups in a time efficient manner; Fig. 5 illustrates 3 possible combinations of assigning three disassembly tasks to the human operator, the robot, and the HRC;

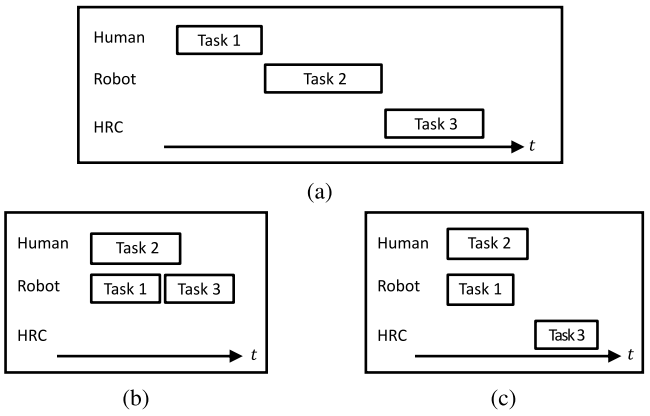

Fig. 5. Example of distribution of three tasks.

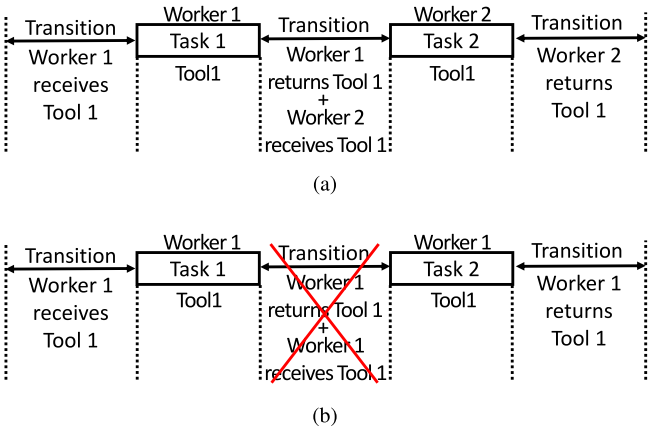

Fig. 6. (a) Task 1 & Task 2 requiring the same tool assign to different workers; (b) Task 1 & Task 2 requiring the same tool assign to the same worker.

Fig. 5(a) is an example of inefficient task distribution in which each task is assigned to one of the worker groups; by contrast, our proposed task planner could distribute the human operator and the robot to different tasks at the same time as illustrated in Figs. 5(b) and 5(c), yielding the time reduction of completing the three tasks.

Next, Constraints (8) to (10) enforce the sequential processing of tasks that violate the safety distance requirement, preventing the human operator and the robot from processing tasks i and j in parallel. For instance, if Task 1 and Task 2 shown in Fig. 5 can be processed by two worker groups simultaneously but belong to set D as an unsafe task pair, the mode in Fig. 5(a) is preferred to avoid simultaneous executions of the two tasks by the human operator and the robot. In other words, only one of the decision variables x_{1w_1t} and x_{2w_2t} can be set to 1 at time t, where w_1 and w_2 denote the human operator and the robot, respectively. Also, M represents a number larger than the latest time point considered in the planning horizon.

Constraint (11) adapts the resource-constrained problem (RCPSP) to limit the quantities of disassembly tools during the planning horizon T. Each tool can only be taken by the human operator or the robot at a time. For example, if Task 1 and Task 2 require different disassembly tools, the modes in Figs. 5(b) and 5(c) could be conducted so that both the human operator and the robot can work on the tasks simultaneously without exceeding the tool limit. That is to say, both the decision variables x_{1w_1t} and x_{2w_2t} become 1 at time t, where w_1 and w_2 represent the robot and the human operator, respectively.

Lastly, the formulation of the transition time is shown in Constraints (12) to (14); Constraints (12) applies the tool-changing time g_w if the worker w after finishing Task i with Tool a must work on the next Task j requiring different Tool b. Otherwise, the tool-changing time g_w will be ignored if the worker w after finishing Task i proceeds to perform Task j with the same Tool a. Two examples of conducting the tool-changing transition are shown in Fig. 6; Fig. 6(a) presents a scenario of two worker groups being assigned to different tasks with the same tool requirement. The scenario shows that the offset between the events of decision variables $x_{1w_1t_1} = 1$ and $x_{2w_2t_2} = 1$ must be larger than the summation of p_{1w_1} (processing time of Task 1 by worker group w_1) and g_w (tool transition time by worker groups w_1 and w_2). On the contrary, Fig. 6(b) shows the same worker group w_1 being assigned to two tasks requiring the same tool, meaning that if the decision variable $x_{1w_1t_1}$ equals 1 at time t_1, the other decision variable $x_{2w_1t_2}$ will become 1 where $t_2 = t_1 + p_{1w_1}$. Thus, no offset between the two tasks. The comparison shows that the transition between Task 1 and Task 2 in Fig. 6(a) is essential, but in Fig. 6(b), the worker group 1 can possess the tool without the tool-changing transition.

Constraints (13) is a supplementary formulation for Constraints (12) that applies the tool-changing time between two sequential tasks assigned to different workers w_1 and w_2 that require the same disassembly tool a. Lastly, Constraints (14) applies the time penalty for performing tasks between task groups. If Task i and Task j do not belong to the same HDD module, a transition time g_w will be carried out to discourage the worker from working back and forth on tasks that belong to different HDD modules.

The features of the proposed sequence planner for the HDD disassembly are highlighted below:

- Distribution of disassembly tasks: The proposed task planner can not only assign one task to one human operator or one robot but also dispatch both the human operator and the robot to the same task as the HRC worker group (see Table 1b).
- Restriction of the maximum number of disassembly workers: The task planner dispatches at each time point at most one human operator and one robot without their being assigned to multiple tasks at the same time.
- Limit in the number of disassembly tools: Different disassembly tasks may require the same disassembly tool. The task planner can prevent the tasks requiring the same tool from being assigned to workers at the same period.
- Precedence relationships among the components: The proposed task planner can enforce the disassembly rule and distribute the tasks without violating the disassembly sequences.
- Dispatch of the robot to unsafe disassembly tasks: If unsafe conditions like sharp edges in components and unsafe distances between nearby disassembly tasks are detected, the proposed task planner can force the robot to perform the unsafe tasks or prevent the tasks from being executed by the human operator and the robot in parallel to avoid collisions between the human operator and the robot.
- The transition time caused by moving between disassembly modules: moving from one disassembly module (as shown in Fig. 4) could lead to a significant delay between disassembly tasks. By conducting it as an optimization problem, the scenario of working back-and-forth on tasks in different disassembly modules should be eliminated. As can be seen in Fig. 7, Worker 1 in Fig. 7(a) spends a longer time working back and forth between the tasks, and the Worker in Fig. 7(b) spends less time moving between the tasks.
- The transition of tool changing and switching tools between workers: the process of receiving and returning the disassembly tool is not necessary and should be flexible. By separating the transition time from the disassembly process, we can concentrate on approximating the processing time of the disassembly task itself and potentially saving the time of tool-changing. Examples of two tool-changing scenarios are illustrated in Fig. 6, in which Worker 1 in Fig. 6(a) must return Tool 1 before Worker 2 starts

Table 2
Properties and required disassembly tasks for all individual HDD components.

Disassembly module	Task No.	Disassembly task	Disassembly actions	Tool required
Actuator module	Task 1	Top Actuator	Pulling out	None
	Task 2	Actuator Arm	Unscrewing	Flat-Head Screwdriver
	Task 3	Bottom Actuator Screw 1	Unscrewing	T6 Torx Screwdriver
	Task 4	Bottom Actuator Screw 2	Unscrewing	T6 Torx Screwdriver
	Task 5	Bottom Actuator Screw 3	Unscrewing	T8 Torx Screwdriver
	Task 6	Bottom Actuator	Picking up	None
Platter module	Task 7	Spindle Screw 1	Unscrewing	T8 Torx Screwdriver
	Task 8	Spindle Screw 2	Unscrewing	T8 Torx Screwdriver
	Task 9	Spindle Screw 3	Unscrewing	T8 Torx Screwdriver
	Task 10	Spindle	Picking up	None
	Task 11	Platter	Picking up	Suction Cup
Chip module	Task 12	Chip Screw 1	Unscrewing	T8 Torx Screwdriver
	Task 13	Chip Screw 2	Unscrewing	T8 Torx Screwdriver
	Task 14	Chip	Picking up	None

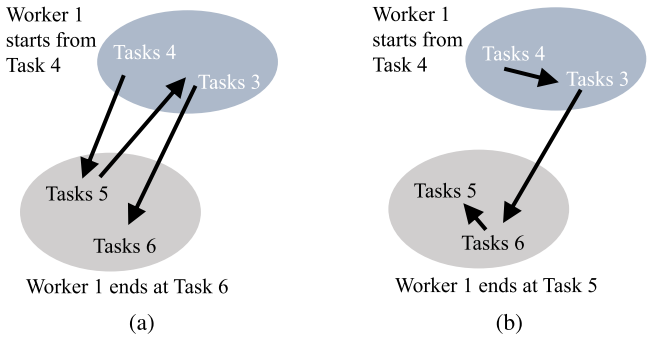

Fig. 7. (a) Undesirable task sequence (b) Desired task sequence.

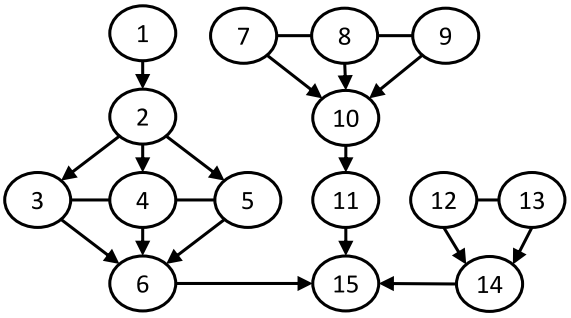

Fig. 8. Precedence relationships of HDD disassembly tasks.

working on Task 2. By contrast, Worker 1 in Fig. 6(a) is assigned to both Task 1 and Task 2 requiring the same tool, so the tool-changing time between the two tasks should be removed since Worker 1 still possesses Tool 1 after performing Task 1.

3. Numerical studies

The purpose of this section is to examine the proposed sequence planner before implementing it to a real product disassembly. A used Seagate HDD is employed to emulate the disassembly sequence with HRC. The used HDD and the disassembled components are exhibited in Fig. 3 and Fig. 4, respectively. The HDD consists of 15 sub-assemblies and their precedence relationships are illustrated in Fig. 8, in which the arrows are pointing from the preceding tasks to the succeeding tasks, noting that the succeeding task will not start until the preceding task finishes. Moreover, the non-directional lines indicate that the tasks being linked together have no precedence relationships and can be performed in parallel by the robot and the human operator. The whole disassembly is complete when Component 1 to Component 14 are all dismantled from Component 15, which is the HDD base. The numerical and experimental studies were carried out on a machine with an Intel Core i7-6700 CPU, 64 GB RAM, an Nvidia GeForce GTX 1050 Ti, and Windows 10 operating system. The proposed disassembly sequence planner was solved using Python language with Python-MIP package and Gurobi optimization solver [78].

The dismantling actions of Component 1 to Component 14 are defined as Task 1 to Task 14, respectively. Each disassembly task involves detaching parts or loosening screws from the HDD base. Depending on the features of the objects to be disassembled, each task can be carried out with or without a tool. Table 2 shows the disassembly task names, actions, and the required tools, with the numbering of the tasks in line with the numbering of the components in Fig. 3.

Each of the disassembly tasks can be executed by one of the three worker groups. Each worker group consumes a different processing time on each disassembly task. The HRC worker group is special because it requires both the human and the robot for the same task, implying that if a task is assigned to HRC, no other tasks can be performed simultaneously. Thus, even though the worker group HRC performs some tasks the fastest among the three worker groups, the tasks will not be assigned to HRC because of taking up both the human operator and the robot during one disassembly process.

For simulation purposes, it is assumed that only one human operator and one robot are employed during the HDD disassembly; the processing time of each worker group is randomly generated and is set to be constant without being affected by the positions of the disassembly tasks in the sequence. The human operator and the robot are both capable of performing the same disassembly tasks and they share the same tools. We also assume the human operator and the robot can work on the assignment individually or work on the same task collaboratively. When the task is assigned to HRC, both the human operator and the robot know their roles in the collaborative task.

Case Study I

In the first case study, we assume that Task 1 is unsafe for human operation. Task 1 is the removal of the top actuator with a strong magnet, so it should be detached by the robot to avoid hand injury. Meanwhile, we assume that the task pairs ((Task 7 & Task 8), (Task 7 & Task 9), (Task 8 & Task 9), and (Task 12 & Task 13)) are too close to be performed by the human operator and the robot in parallel. These task pairs are formulated as the set D in Constraints (8) to (10). Additionally, the virtual processing time and transition time of the three worker groups are listed in Table 3 and Table 4, respectively. The processing time for each disassembly is randomly generated between three and ten seconds. Each disassembly task requires different tools as

Table 3
Case Study I: Disassembly time.

Task No.	Processing time		
	Human	Robot	HRC
Task 1	10	8	3
Task 2	10	8	3
Task 3	10	8	3
Task 4	3	4	6
Task 5	3	4	6
Task 6	10	8	3
Task 7	10	8	3
Task 8	3	6	4
Task 9	3	6	4
Task 10	8	10	3
Task 11	10	8	3
Task 12	3	6	4
Task 13	8	10	3
Task 14	10	8	3

Table 4
Case Study I: Transition time.

Worker	Transition time (s)
Human	1
Robot	2
HRC	2

Table 5
Tools represented by symbols.

Tool name	Symbol
Flat-Head Screwdriver	△
T6 Torx Screwdriver	□
T8 Torx Screwdriver	◇
Suction Cup	○

shown in Table 2 and can be carried out by one of the three worker groups with distinctive processing time.

The disassembly sequence starts from Task 7 requiring T8 Torx screwdriver. Task 7 is assigned to HRC group. The first two transitions occur from Task 7 to Task 12 by the human operator and from Task 7 to Task 1 by the robot. It is because the HRC group needs time to return the tool and to move from Platter Module (red) to the other disassembly modules (Chip Module in blue and Actuator Module in yellow). In addition, since Task 12 and Task 13 require the same tool, the human operator can work on the two tasks without tool-changing. The human operator then takes one second to return the tool and to move to the next task between the fifteen and sixteen seconds in the timeline in Fig. 10. Afterward, the HRC group is selected to perform Task 2 with the flat-head screwdriver due to the lowest disassembly time. After a one-second transition of moving between disassembly modules, the human operator proceeds to work on Task 9 and Task 8 in Platter Module using the same tool, and then transits to Task 5 in Actuator Module with the same tool. In the meantime, the robot spends two seconds for tool changing and then performs Task 3 from the twenty-one second to twenty-nine seconds in the timeline. Next, Task 14 is executed by HRC between the thirty-one and thirty-four second after a one-second transition of the human operator, and a two-second transition of the robot, as shown in Table 4. Then, the human operator spends one second moving from Task 14 to Task 4 with T6 Torx screwdriver. Task 6 is performed by the robot after Task 4 because of the precedence relationships between the two tasks. While Task 6 is processed by the robot, the human operator performs Task 10 after a one-second transition between thirty-eight and thirty-nine seconds in the time frame. Finally, after one-second and two-second transition by the human operator and the robot respectively, Task 11 is executed by HRC.

Fig. 9 shows the search process of the optimal sequence with minimum disassembly time. The minimum disassembly time is obtained

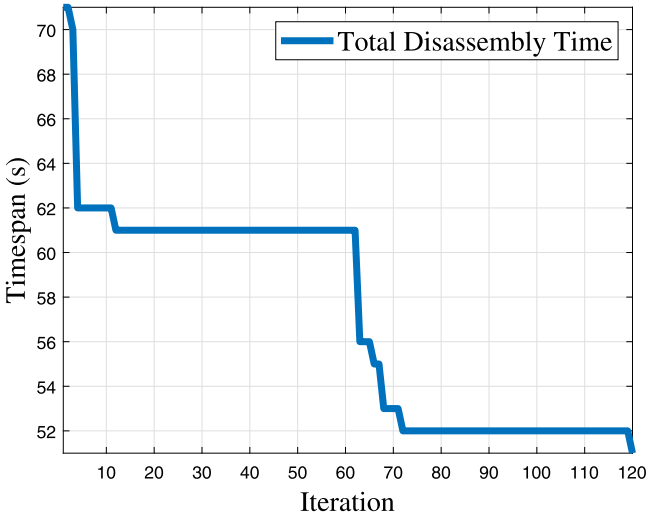

Fig. 9. Case Study I: Search process of optimal sequence with minimum disassembly time.

by a linear programming optimizer using dual-simplex method after 120 iterations; the optimizer firstly found a feasible sequence with 71 s, then continued to search for the other feasible sequences having smaller disassembly time. After 383 s of searching for the minimum total disassembly time, the optimizer stopped searching after no other disassembly sequence can be found with less than 51-second total disassembly time for the HDD. Fig. 10 shows the result of the optimal disassembly sequence with 51-second total disassembly time; the color represents the HDD modules in Fig. 4 and the symbols '△', '□', '◇', and '○' (see Table 5) indicate the tools used in the tasks, noting that the tasks without any symbols do not need any tools.

It can be seen from the first simulation, the unsafe Task 1 is successfully assigned to the robot to avoid potential human injury. Meanwhile, the task pairs of Task 7 & Task 8, Task 8 & Task 9, Task 7 & Task 9, and Task 12 & Task 13 are not simultaneously performed by the human operator and the robot, yielding a safe working distance between the human and the robot. The case study also successfully demonstrates the transition time caused by tool-changing and moving between different disassembly modules.

Case Study II

In the second study, we assume that Task 2 is unsafe for human operation, and to compare with the first case study, the task pairs are reduced to (Task 12 & Task 13) which is unsafe for the human operator and the robot working in parallel. The processing time for each disassembly is also randomly generated as three to ten seconds. The required tools and transition time remain the same as in Case Study I. The transition time and the virtual processing time of the human operator, the robot, and the HRC are listed in Table 4 and Table 6, respectively.

Fig. 11 shows the search process of the optimal sequence with minimum disassembly time. The minimum disassembly time is obtained after 127 iterations. Similar to the sequence search pattern of Case I, the optimizer firstly found a feasible sequence with a large disassembly time, then continued to search for the other feasible sequences with time less than 69 s. It took 275 s to search for the minimum total disassembly time. The optimizer stopped searching after no other disassembly sequence can be found with less than 49-second total disassembly time for the HDD. Fig. 10 shows the result of the optimal disassembly sequence with 49-second total disassembly time; Fig. 12 demonstrates the Gantt diagram of the optimal HDD disassembly sequence of Case Study II. The unsafe Task 2 is assigned to the robot,

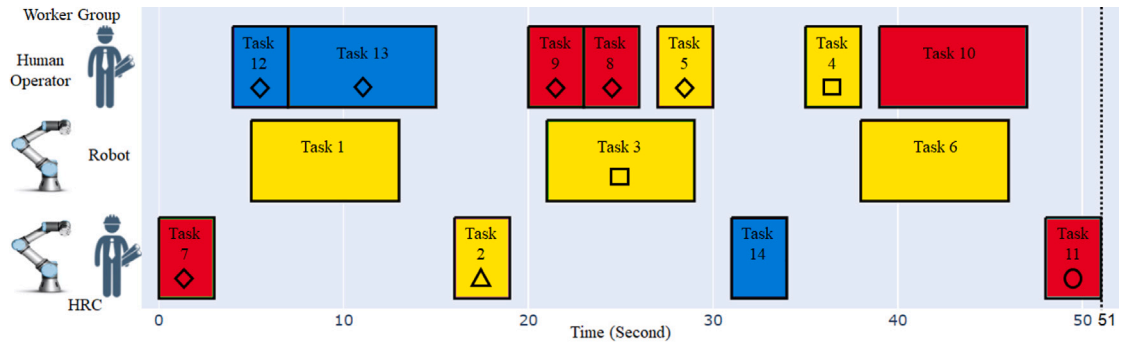

Fig. 10. Case Study I: Gantt chart of optimized disassembly sequence (Colors and Symbols defined in Fig. 4 and Table 5). (For interpretation of the references to color in this figure legend, the reader is referred to the web version of this article.)

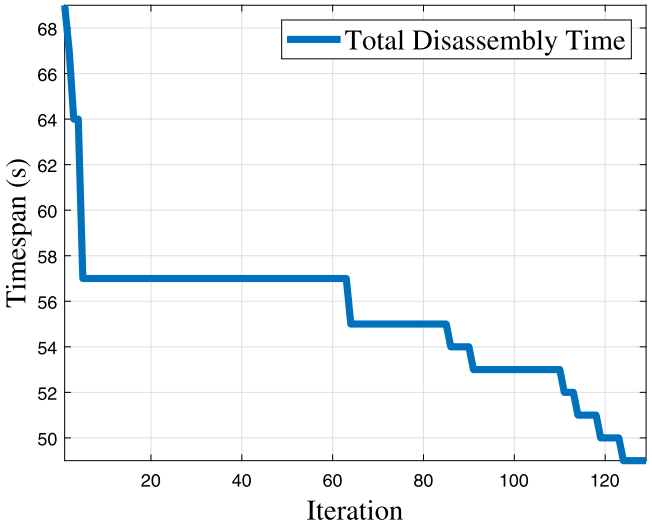

Fig. 11. Case Study II: Search process of optimal sequence with minimum disassembly time.

Table 6
Case Study II: Disassembly time.

	Processing time (s)		
Task No.	Human	Robot	HRC
Task 1	3	9	7
Task 2	3	10	2
Task 3	9	6	3
Task 4	9	6	3
Task 5	10	7	3
Task 6	9	3	6
Task 7	7	10	3
Task 8	7	10	3
Task 9	7	10	3
Task 10	10	8	5
Task 11	8	10	3
Task 12	3	10	9
Task 13	3	10	9
Task 14	4	9	6

and the task pair (Task 12 & Task 13) is not performed simultaneously by the human operator and the robot. The colors (red, yellow and blue) represent the tasks that belong to different disassembly modules, and the symbols ('△', '□', '◇' and '○') represent different tools used in the tasks.

The disassembly sequence starts from HRC being assigned to Task 7, Task 8 and Task 9 sequentially. Because the three tasks require the same tool, no transition time is required in-between. Next, the human operator performs Task 1 without any tool after a one-second transition from Task 7, and then the worker takes another one-second transition to Task 10 in another disassembly module. Meanwhile, Task 2 is performed by the robot after the completion of Task 1 because of the precedence relationships between Task 1 and Task 2. Afterward, Task 5 is executed by HRC between the twenty-five and twenty-eight seconds in the timeline following a one-second transition of the human operator and a two-second transition of the robot. Next, after taking a one-second transition, the human operator performs Task 12 and Task 13 continuously using the same T8 Torx screwdriver and then transits to Task 14 without tools. In the meantime, the robot takes a two-second transition to perform Task 3 and Task 4 non-preemptively using the same T6 Torx screwdriver. Finally, Task 6 is performed by the robot from forty-four to forty-seven seconds, and Task 11 is performed by the human operator between forty-one and forty-nine seconds. The total HDD disassembly is complete at forty-nine seconds after the completion of Task 11.

The second simulation shows that Task 2 is successfully assigned to the robot to avoid human injury. Meanwhile, the task pair of (Task 12 & Task 13) is performed by the human operator sequentially, preventing collision between the human operator and the robot. The transitions are successfully implemented for the tool-changing from Task 7 to Task 1, and from Task 13 to Task 14, and the moving from Task 1 to Task 10, and from Task 10 to Task 5, and etc.

4. Experimental studies

This section presents the validation of the proposed disassembly sequence planner via experimental studies. The goals are: (1) to disassemble all the components on the HDD considering human–robot collaboration, (2) to minimize the total disassembly time with minimum transitions, (3) to prevent human injury, and (4) to comply with tool constraint. The experimental setup is shown in Fig. 13, which contains a human operator, a six-degree-of-freedom manipulator (the robot), a disassembly toolset, and requisite cameras.

The HDD disassembly is composed of 14 individual tasks. Task 1 is considered unsafe for human operation, as the removal of the top actuator with a strong magnet requires a large force that could cause human injury. All the HDD components, that are identified using machine learning methods [79–81], are assumed to be reachable by both the human operator and the robot. Additionally, the task pairs ((Task 7 & Task 8), (Task 8 & Task 9), (Task 7 & Task 9), and (Task 12 & Task 13)) do not satisfy the minimum safety distance, as illustrated in Fig. 16. These task pairs are formulated as the set D in Constraints (8) to (10) to prevent the human and the robot from working in parallel. The precedence relationships of the disassembly tasks and the disassembly process are conducted by empirical methods. The disassembly actions and the required tools are shown in Table 2, in which one T6 Torx screwdriver, one T8 Torx screwdriver, one flat-head screwdriver, and one suction cup are prepared for the disassembly tasks. The processing time of the disassembly tasks and the transition time of the three

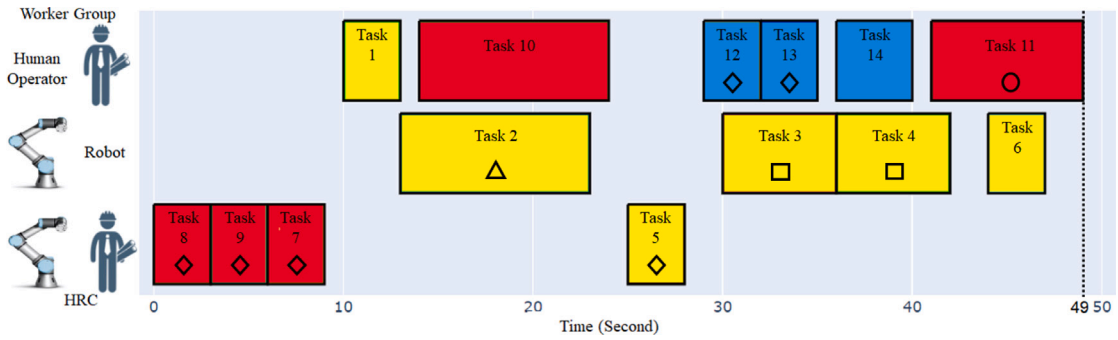

Fig. 12. Case Study II: Gantt chart of optimized disassembly sequence (Colors and symbols defined in Fig. 4 and Table 5). (For interpretation of the references to color in this figure legend, the reader is referred to the web version of this article.)

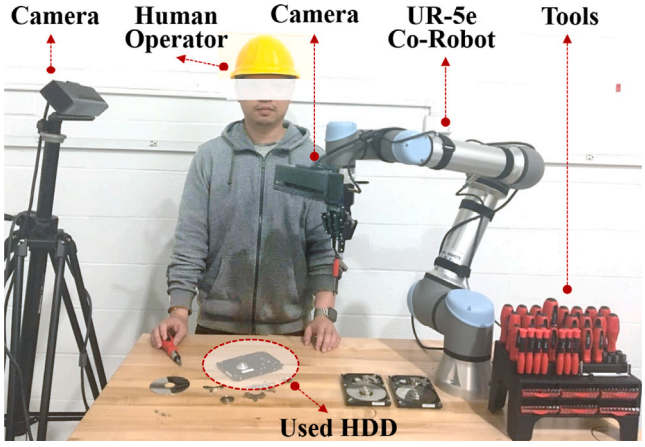

Fig. 13. Experiment test setup.

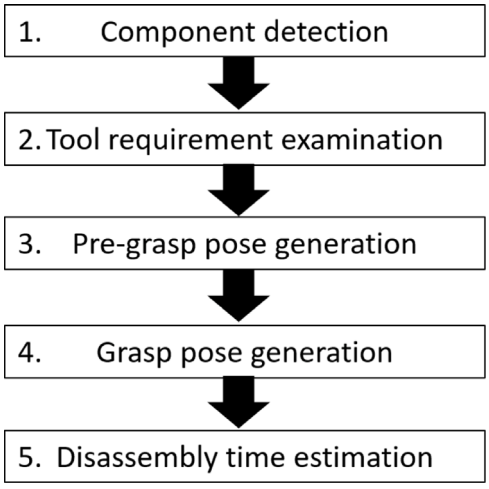

Fig. 14. Flow chart of disassembly time calculation.

worker groups are listed in Table 7 and Table 8, respectively. Please note tasks with the disassemble time of 99 s denote their impossibilities of completion by corresponding worker groups. The worker group's disassembly time of each task is calculated following the flow chart in Fig. 14, where the pre-grasp and grasp poses are demonstrated in Fig. 15 in which we assume the component can be freely detached along the vertical direction. Noting that since the proposed task planner is already complex, the disassembly direction is simplified and the disassembly actions (see Table 2) are limited to pulling out, unscrewing and picking up. The completion time of each task and the transition time used in the experimental studies are obtained by preliminary tests, in which the processing time of each disassembly task and the transition by the three worker groups are recorded. Furthermore, the human operator has the dominant control in the disassembly process; the robot will engage in assigned disassembly tasks only after its end-effector is tapped by the human operator. This configuration also guarantees human safety in the whole HDD disassembly.

Fig. 17 and Fig. 18 show the search process of the total disassembly time and the Gantt diagram of the optimal HDD disassembly sequence, respectively. The minimum disassembly time is obtained after 189 iterations. The sequence search pattern is similar to Case I and Case II; a feasible sequence was initially found with a large disassembly time (203 s), then the optimizer continued to search for the other feasible sequences with shorter time. The optimizer stopped searching after no other disassembly sequence can be found with less than 151-second total disassembly time for the HDD. The search process takes 1349 s, which is longer than the ones from the two numerical studies due to longer processing time by the worker groups in the real world. Fig. 10 shows the result of the optimal disassembly sequence with 151-second total disassembly time; The disassembly process begins after the HDD

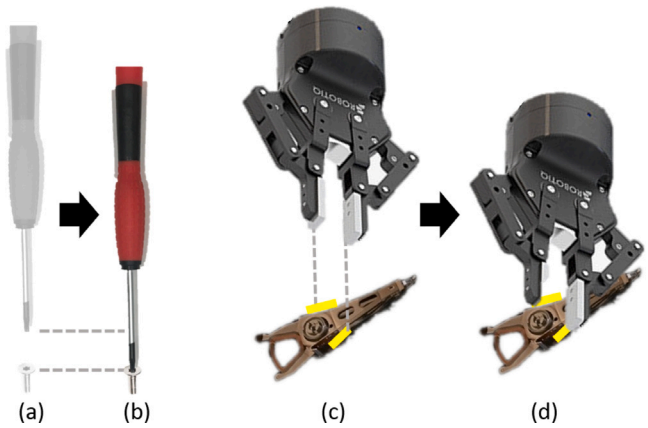

Fig. 15. Demonstration of Pre-grasp and Grasp Poses: (a) pre-grasp position for a task requiring a screwdriver; (b) grasp position for a task requiring a screwdriver; (c) pre-grasp position for robot assigned to a task without requiring a tool; (d) grasp position for robot assigned to a task without requiring a tool. Note that the yellow lines indicate the grasp position of the robot. (For interpretation of the references to color in this figure legend, the reader is referred to the web version of this article.)

is placed on the workbench, as shown in Fig. 19. A recycling zone for placing the disassembled components is designed on the bottom left of the workbench. Both the human operator and the robot will place the disassembled components in the designated area. The toolset is placed near the base of the manipulator. The human operator and the robot

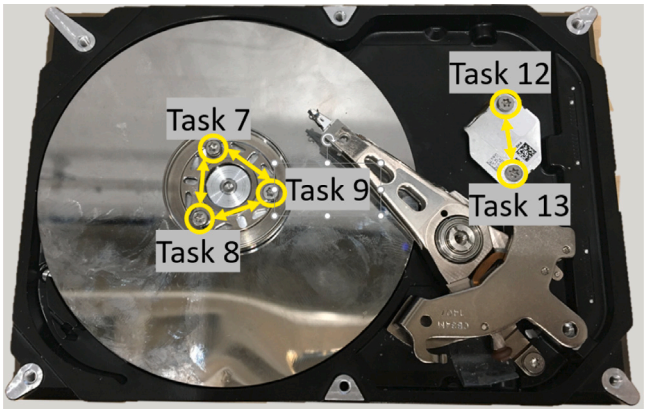

Fig. 16. Tasks not satisfying minimum safety distance.

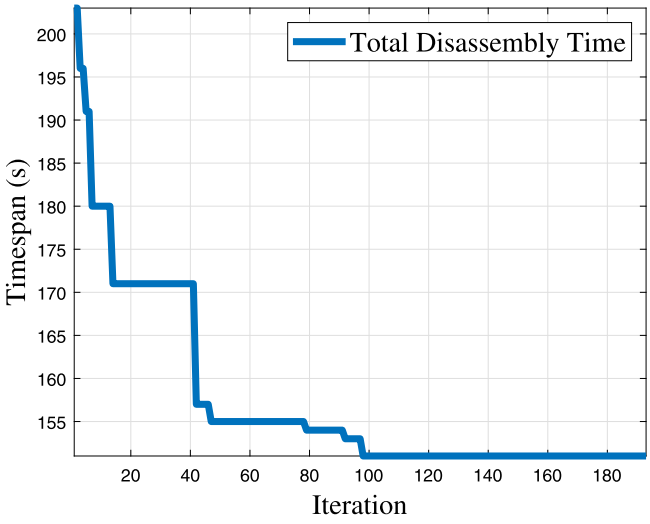

Fig. 17. Experiment: Search process of optimal sequence with minimum disassembly time.

Table 7
Experiment: Processing time of disassembly tasks.

Task No.	Processing time (s)		
	Human	Robot	HRC
Task 1	22	26	15
Task 2	16	99	25
Task 3	14	99	99
Task 4	14	99	99
Task 5	15	99	99
Task 6	14	11	99
Task 7	12	99	99
Task 8	12	99	99
Task 9	12	99	99
Task 10	15	9	22
Task 11	23	99	13
Task 12	12	99	99
Task 13	12	99	99
Task 14	11	13	7

Table 8
Experiment: Transition time.

Worker	Transition time (s)
Human	2
Robot	4
HRC	4

must return the tool only if the current task and the next task require different tools.

After the initialization, the human operator and the robot proceed to work on Task 7–9 and Task 1, respectively. Because Tasks 7 to 9 require the same type of T6 Torx screwdriver, the human operator can work on these tasks continuously without returning the tool during the three tasks, as shown in Fig. 20. In addition, although the robot processes Task 1 slower than the human operator (26 s v.s. 22 s), the robot is assigned to perform Task 1 because it is marked as unsafe for human operation at the initialization stage. The robot returns to its initial position after placing the top actuator part to the recycling zone at around 26 s. Meanwhile, the human operator after placing the screws to the recycling zone proceeds to return the T6 Torx screwdriver and then grab the flat-head screwdriver for Task 2. It is worth noting that the tool-changing time is presented between Task 7 and Task 2 for 2 s.

After the human operator finishes exchanging the tool, Task 2 and Task 10 are assigned to the human operator and the robot, as shown in Fig. 21. The human operator and the robot are working on the two tasks in parallel during forty-three to fifty-two seconds, noting that Task 2 and Task 10 belong to different disassembly modules (referring to Fig. 4) and do not have direct precedence relationships. After the two parallel tasks are complete, the human operator and the robot take 2 s and 4 s respectively to be ready for the next task, which is assigned to HRC.

Next, the HRC is assigned to Task 11, the removal of the platter shown in Fig. 22. The platter is flat and too thin to be removed easily by hand, so the suction cup is required to be deployed first by the human operator, and then the robot grabs the holder part of the suction cup to remove the platter from the HDD base. After the platter successfully landed on the recycling area, the human operator must help detach the suction cup from the platter since the robot is incapable to detach the platter by itself.

After returning the suction cup between sixty-nine and seventy-one seconds, the human operator is ready for the next tasks shown in Fig. 23. The next three tasks are composed of Task 5 requiring a T8 Torx screwdriver and Task 3 & Task 4 requiring a T6 Torx screwdriver. The task planner also successfully displays the tool-changing time between eighty-six and eighty-eight seconds. It should be noted that Task 5, Task 3 and Task 4 do not have precedence relationships, but these tasks must be complete before Task 6, as illustrated in Fig. 8.

After the human operator returns the tool for Task 4, the robot and the human operator are again assigned to distinctive tasks synchronously, as shown in Fig. 24. The robot is assigned to Task 6 to remove the bottom actuator from the 118 to 129 s. Meanwhile, the human operator is assigned to Task 13 and Task 12 between 118 and 142 s to remove the screws on the control chip, which is Task 14. Similar to Task 3 & Task 4, Task 13 & Task 12 require the same tool, so there is no tool-changing time between Task 13 & Task 12.

The last remaining task is Task 14 that is assigned to HRC shown in Fig. 25. The human operator after performing Task 12 has sufficient time to return and be ready for Task 14, the control chip removal. The grasping position of the chip is thin and sharp, and the chip is stuck on the surface of the HDD base, so the disassembly process requires HRC; the human operator holds the bottom of the HDD so that the robot can pull the chip out of the HDD base. The total disassembly is complete at 151 s after the chip is removed.

The experiment and the two simulations in the previous section show the potential of conducting the HDD disassembly with human–robot collaboration. The proposed problem formulation successfully prevents the tasks that do not meet the minimum safety distance from being assigned to the human operator and the robot in parallel. The task planner also prevents the unsafe tasks from being assigned to the human operator in spite of the inferior disassembly time by the robot. The transitions, including the tool-changing time, tool-changing penalty and the disassembly module switching time are successfully conducted in the disassembly scheduling. The tool limit and the precedence relationships of the tasks are also considered explicitly during the whole disassembly. The experiment video is available via this link.

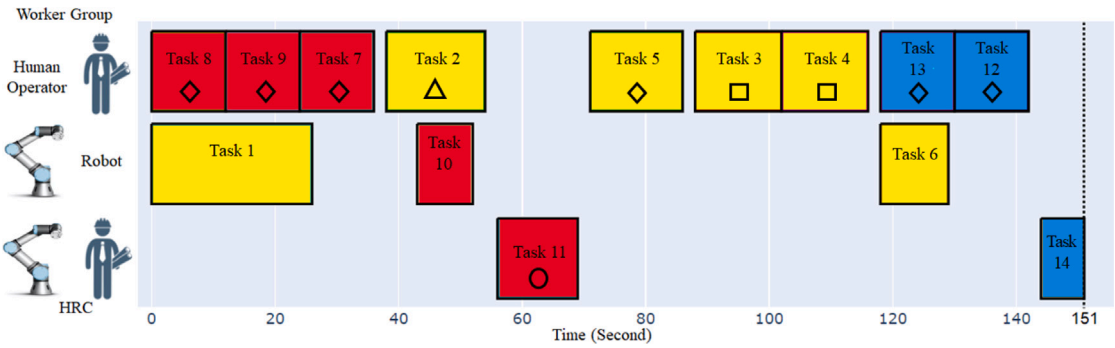

Fig. 18. Experiment: Gantt chart of optimized disassembly sequence (Colors and symbols defined in Fig. 4 and Table 5). The experimental test video is available as the supplemental materials. It is also available via this link. (For interpretation of the references to color in this figure legend, the reader is referred to the web version of this article.)

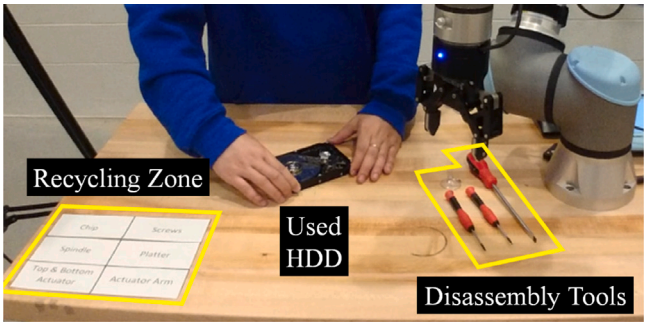

Fig. 19. Initialization of the HDD disassembly.

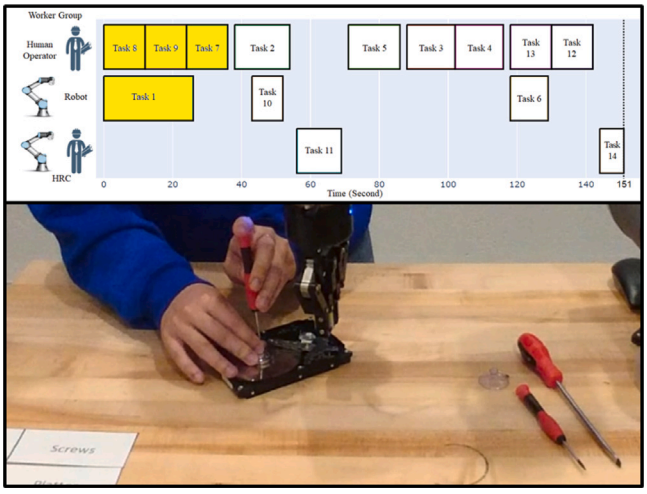

Fig. 20. Human operator performs Tasks 7–9 during 0–36 s, and robot performs Task 1 during 0–26 s.

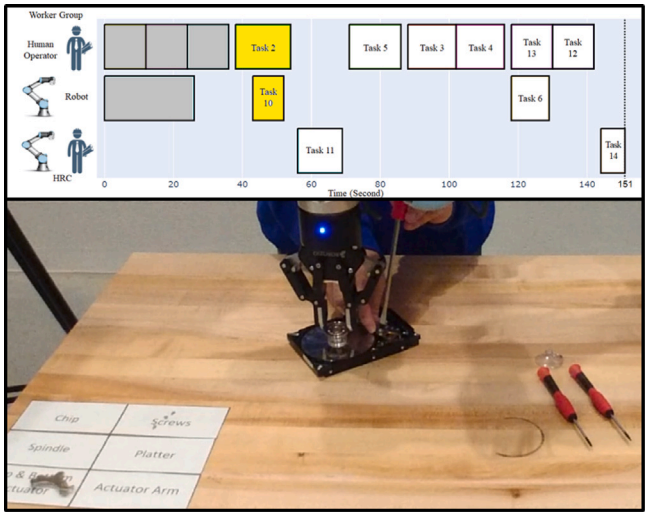

Fig. 21. Human operator performs Tasks 2 during 38–54 s, and robot performs Task 10 during 43–52 s.

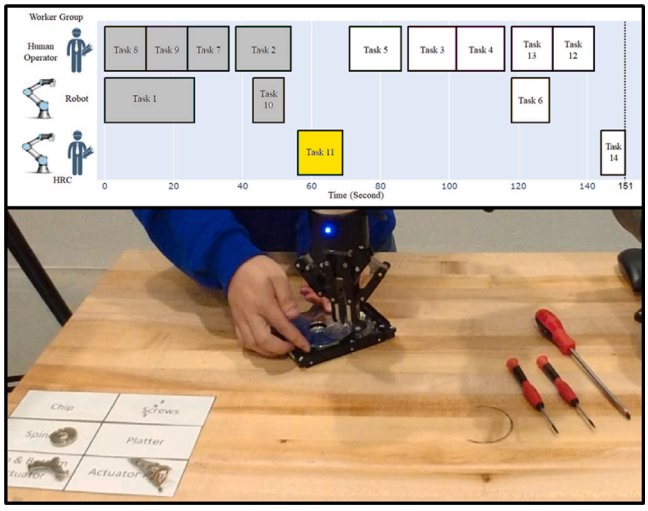

Fig. 22. Human operator and robot (HRC) perform Tasks 11 during 56–69 s.

5. Conclusions and future research

This paper presents the formulation of a disassembly sequence planning problem in HRC setting into an optimization problem. The proposed sequence planner is capable of minimizing the total disassembly time and assigning the human and the robot to not only sequential or parallel tasks but also assign them together as a team. The unsafe condition of the components of the e-waste and the minimum distance between the disassembly tasks are also conducted as constraints in the optimization problem to prevent unsafe disassembly operations. In addition, the transitions, including the tool-changing time and the disassembly module switching time, are explicitly considered in this paper. Case studies have been carried out to demonstrate the proposed disassembly task planner with various scenarios of the disassembly workers with different processing periods and safe conditions. Both numerical and experimental tests show that the human operator and the robot accomplish the disassembly tasks collaboratively without violating the disassembly rules and the safety constraints.

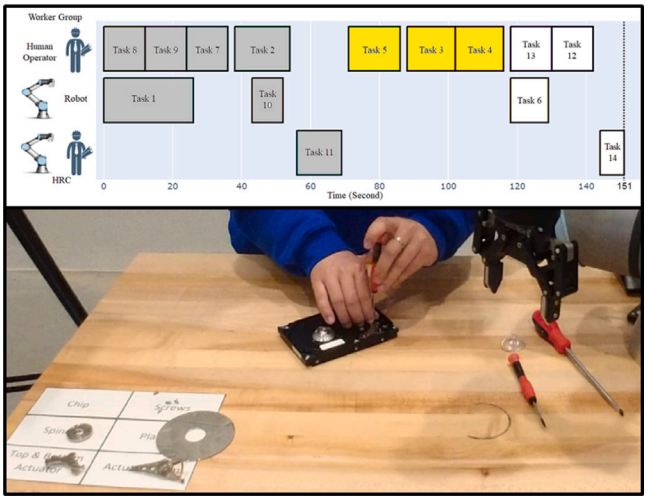

Fig. 23. Human operator performs Tasks 5, Task 3 & Task 4 during 71–116 s.

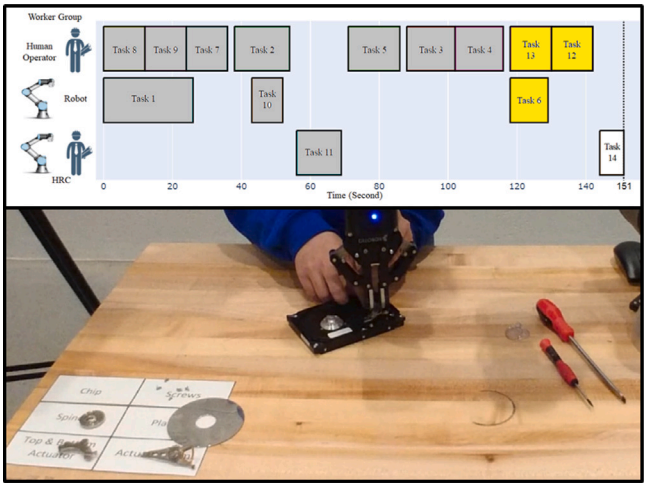

Fig. 24. Human operator performs Tasks 12 & Task 13 during 118–142 s, and robot performs Task 6 during 118–129 s.

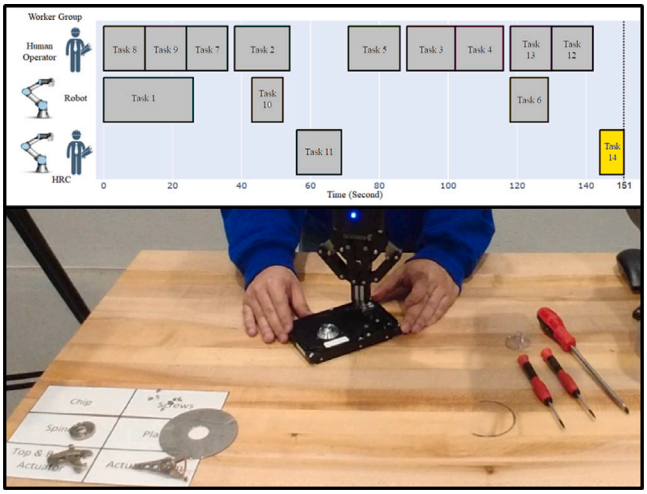

Fig. 25. Human operator and robot (HRC) perform Tasks 14 during 144–151 s.

It is worth noting that there are still limitations in our research. First, the disassembly time of the components needs to be obtained through evaluations or historical experience data before disassembly. Second, the disassembly time variation caused by the deformation or deterioration of components has not been considered; we have assumed that the components with the same type and size will have identical conditions, unless the component is categorized as unsafe for human operation. Third, even though the unsafe condition of the component is successfully formulated as constraints in the problem formulation, the method of identifying the component conditions is not well defined. Fourth, our study only considers the efficiency of the disassembly. The labor cost, the energy consumption and the value of parts, however, are ignored. Fifth, so far we have only applied a few models of HDDs for the disassembly experiment. More experiments with extensive varieties of HDDs should be conducted to develop a more general problem formulation. In addition, the numerical optimization problem is manually generated. According to the extensive literature review as well as our best knowledge, no existing studies have achieved the automatic generation of the numerical optimization problem for disassembly while considering the above-mentioned scenarios. It is a very challenging yet interesting problem that we would like to explore as our future work.

CRediT authorship contribution statement

Meng-Lun Lee: Algorithm development, Programming, numerical and experimental studies, Writing – original draft. **Sara Behdad:** Supervision on remanufacturing and problem formulation, Writing – review & editing. **Xiao Liang:** Supervision on optimization, Writing – review & editing. **Minghui Zheng:** Oversight and leadership responsibility for the research activity planning and execution, Supervision on algorithm development as well as numerical and experimental studies, Writing – review & editing.

Declaration of competing interest

The authors declare that they have no known competing financial interests or personal relationships that could have appeared to influence the work reported in this paper.

Acknowledgment

This material is based upon work supported by the National Science Foundation - USA under Grants No. 2026533, No. 2026276, and No. 1928595. Any opinions, findings, and conclusions or recommendations expressed in this material are those of the authors and do not necessarily reflect the views of the National Science Foundation.

Appendix A. Supplementary data

Supplementary material related to this article can be found online at https://doi.org/10.1016/j.rcim.2021.102306.

References

[1] B.H. Robinson, E-waste: an assessment of global production and environmental impacts, Sci. Total Environ. 408 (2) (2009) 183–191.
[2] Y. Ren, C. Zhang, F. Zhao, G. Tian, W. Lin, L. Meng, H. Li, Disassembly line balancing problem using interdependent weights-based multi-criteria decision making and 2-optimal algorithm, J. Cleaner Prod. 174 (2018) 1475–1486.
[3] M.W. McIntosh, B. Bras, Determining the value of remanufacture in an integrated manufacturing-remanufacturing organization, in: International Design Engineering Technical Conferences and Computers and Information in Engineering Conference, Vol. 80340, American Society of Mechanical Engineers, 1998, V004T04A037.
[4] V. Suresh, W. Liu, M. Zheng, B. Li, High-resolution structured light 3D vision for fine-scale characterization to assist robotic assembly, in: Dimensional Optical Metrology and Inspection for Practical Applications X, Vol. 11732, International Society for Optics and Photonics, 2021, p. 1173203.
[5] A.F. Lambert, S.M. Gupta, Disassembly Modeling for Assembly, Maintenance, Reuse and Recycling, CRC Press, 2004.

[6] D.N. Perkins, M.-N.B. Drisse, T. Nxele, P.D. Sly, E-waste: a global hazard, Ann. Global Health 80 (4) (2014) 286–295.

[7] Y. Tang, M. Zhou, M. Gao, Fuzzy-Petri-net-based disassembly planning considering human factors, IEEE Trans. Syst. Man Cybern.-Part A: Syst. Hum. 36 (4) (2006) 718–726.

[8] E. Kongar, S.M. Gupta, Disassembly sequencing using genetic algorithm, Int. J. Adv. Manuf. Technol. 30 (5–6) (2006) 497–506.

[9] S.-K.S. Fan, C. Fan, J.-H. Yang, K.F.-R. Liu, Disassembly and recycling cost analysis of waste notebook and the efficiency improvement by re-design process, J. Cleaner Prod. 39 (2013) 209–219.

[10] S.M. McGovern, S.M. Gupta, Unified assembly-and disassembly-line model formulae, J. Manuf. Technol. Manag. (2015).

[11] T. De Fazio, D. Whitney, Simplified generation of all mechanical assembly sequences, IEEE J. Robot. Autom. 3 (6) (1987) 640–658.

[12] C. Wang, M. Zheng, Z. Wang, C. Peng, M. Tomizuka, Robust iterative learning control for vibration suppression of industrial robot manipulators, J. Dyn. Syst. Meas. Control 140 (1) (2018) 011003.

[13] C. Wang, M. Zheng, Z. Wang, M. Tomizuka, Robust two-degree-of-freedom iterative learning control for flexibility compensation of industrial robot manipulators, in: 2016 IEEE International Conference on Robotics and Automation, ICRA, IEEE, 2016, pp. 2381–2386.

[14] Z. Zheng, W. Xu, Z. Zhou, D.T. Pham, Y. Qu, J. Zhou, Dynamic modeling of manufacturing capability for robotic disassembly in remanufacturing, Procedia Manuf. 10 (2017) 15–25.

[15] J. Huang, D.T. Pham, Y. Wang, M. Qu, C. Ji, S. Su, W. Xu, Q. Liu, Z. Zhou, A case study in human–robot collaboration in the disassembly of press-fitted components, Proc. Inst. Mech. Eng. B 234 (3) (2020) 654–664.

[16] M. Hedelind, S. Kock, Requirements on flexible robot systems for small parts assembly: A case study, in: 2011 IEEE International Symposium on Assembly and Manufacturing, ISAM, IEEE, 2011, pp. 1–7.

[17] S. Hjorth, D. Chrysostomou, Human–robot collaboration in industrial environments: A literature review on non-destructive disassembly, Robot. Comput.-Integr. Manuf. 73 (2022) 102208.

[18] L.P. Berg, S. Behdad, J.M. Vance, D. Thurston, Disassembly sequence evaluation using graph visualization and immersive computing technologies, in: ASME 2012 International Design Engineering Technical Conferences and Computers and Information in Engineering Conference, American Society of Mechanical Engineers Digital Collection, 2013, pp. 1351–1359.

[19] A.C. Lin, T. C. Chang, An integrated approach to automated assembly planning for three-dimensional mechanical products, Int. J. Prod. Res. 31 (5) (1993) 1201–1227.

[20] C. Friedrich, A. Lechler, A. Verl, A planning system for generating manipulation sequences for the automation of maintenance tasks, in: 2016 IEEE International Conference on Automation Science and Engineering, CASE, IEEE, 2016, pp. 843–848.

[21] S. Vongbunyong, M. Pagnucco, S. Kara, Vision-based execution monitoring of state transition in disassembly automation, Int. J. Autom. Technol. 10 (5) (2016) 708–716.

[22] M. Bdiwi, A. Rashid, M. Putz, Autonomous disassembly of electric vehicle motors based on robot cognition, in: 2016 IEEE International Conference on Robotics and Automation, ICRA, IEEE, 2016, pp. 2500–2505.

[23] Q. Lu, Y. Ren, H. Jin, L. Meng, L. Li, C. Zhang, J.W. Sutherland, A hybrid metaheuristic algorithm for a profit-oriented and energy-efficient disassembly sequencing problem, Robot. Comput.-Integr. Manuf. 61 (2020) 101828.

[24] Y. Tang, M. Zhou, E. Zussman, R. Caudill, Disassembly modeling, planning and application: a review, in: Proceedings 2000 ICRA. Millennium Conference. IEEE International Conference on Robotics and Automation. Symposia Proceedings (Cat. No. 00CH37065), Vol. 3, IEEE, 2000, pp. 2197–2202.

[25] A. Lambert, Generation of assembly graphs by systematic analysis of assembly structures, IFAC Proc. Vol. 35 (1) (2002) 85–90.

[26] E.R. Gansner, E. Koutsofios, S.C. North, K.-P. Vo, A technique for drawing directed graphs, IEEE Trans. Softw. Eng. 19 (3) (1993) 214–230.

[27] A.J. Lambert, Determining optimum disassembly sequences in electronic equipment, Comput. Ind. Eng. 43 (3) (2002) 553–575.

[28] K.E. Moore, A. Güngör, S.M. Gupta, Petri net approach to disassembly process planning for products with complex AND/OR precedence relationships, European J. Oper. Res. 135 (2) (2001) 428–449.

[29] M. Zhou, K. Venkatesh, Modeling, Simulation, and Control of Flexible Manufacturing Systems: A Petri Net Approach, World Scientific, 1999.

[30] D. Navtn-Chandra, The recovery problem in product design, J. Eng. Des. 5 (1) (1994) 65–86.

[31] W. Sheng, N. Xi, M. Song, Y. Chen, Robot path planning for dimensional measurement in automotive manufacturing, J. Manuf. Sci. Eng. 127 (2) (2005) 420–428.

[32] V. Van Peteghem, M. Vanhoucke, An experimental investigation of metaheuristics for the multi-mode resource-constrained project scheduling problem on new dataset instances, European J. Oper. Res. 235 (1) (2014) 62–72.

[33] I.A. Chaudhry, A.A. Khan, A research survey: review of flexible job shop scheduling techniques, Int. Trans. Oper. Res. 23 (3) (2016) 551–591.

[34] H. Wang, Flexible flow shop scheduling: optimum, heuristics and artificial intelligence solutions, Expert Syst. 22 (2) (2005) 78–85.

[35] A.J. Lambert, Disassembly sequencing: a survey, Int. J. Prod. Res. 41 (16) (2003) 3721–3759.

[36] X. Liu, G. Peng, X. Liu, Y. Hou, Disassembly sequence planning approach for product virtual maintenance based on improved max–min ant system, Int. J. Adv. Manuf. Technol. 59 (5) (2012) 829–839.

[37] K. Meng, P. Lou, X. Peng, V. Prybutok, An improved co-evolutionary algorithm for green manufacturing by integration of recovery option selection and disassembly planning for end-of-life products, Int. J. Prod. Res. 54 (18) (2016) 5567–5593.

[38] M.R. Bahubalendruni, V.P. Varupala, Disassembly sequence planning for safe disposal of end-of-life waste electric and electronic equipment, Nat. Acad. Sci. Lett. 44 (3) (2021) 243–247.

[39] M. Daneshmand, F. Noroozi, C. Corneanu, F. Mafakheri, P. Fiorini, Industry 4.0 and prospects of circular economy: A survey of robotic assembly and disassembly, 2021, arXiv preprint arXiv:2106.07270.

[40] H.-J. Kim, D.-H. Lee, P. Xirouchakis, Disassembly scheduling: literature review and future research directions, Int. J. Prod. Res. 45 (18–19) (2007) 4465–4484.

[41] M.A. Ilgin, G.T. Taşoğlu, Simultaneous determination of disassembly sequence and disassembly-to-order decisions using simulation optimization, J. Manuf. Sci. Eng. 138 (10) (2016).

[42] T. Go, D. Wahab, M.A. Rahman, R. Ramli, A. Hussain, Genetically optimised disassembly sequence for automotive component reuse, Expert Syst. Appl. 39 (5) (2012) 5409–5417.

[43] S.M. McGovern, S.M. Gupta, A balancing method and genetic algorithm for disassembly line balancing, European J. Oper. Res. 179 (3) (2007) 692–708.

[44] O. Hazır, A. Dolgui, A review on robust assembly line balancing approaches, IFAC-PapersOnLine 52 (13) (2019) 987–991.

[45] E. Özceylan, C.B. Kalayci, A. Güngör, S.M. Gupta, Disassembly line balancing problem: a review of the state of the art and future directions, Int. J. Prod. Res. 57 (15–16) (2019) 4805–4827.

[46] H. Shan, S. Li, J. Huang, Z. Gao, W. Li, Ant colony optimization algorithm-based disassembly sequence planning, in: 2007 International Conference on Mechatronics and Automation, IEEE, 2007, pp. 867–872.

[47] L.-P. Ding, Y.-X. Feng, J.-R. Tan, Y.-C. Gao, A new multi-objective ant colony algorithm for solving the disassembly line balancing problem, Int. J. Adv. Manuf. Technol. 48 (5–8) (2010) 761–771.

[48] C.B. Kalayci, S.M. Gupta, A particle swarm optimization algorithm with neighborhood-based mutation for sequence-dependent disassembly line balancing problem, Int. J. Adv. Manuf. Technol. 69 (1–4) (2013) 197–209.

[49] Y. Gao, Q. Wang, Y. Feng, H. Zheng, B. Zheng, J. Tan, An energy-saving optimization method of dynamic scheduling for disassembly line, Energies 11 (5) (2018) 1261.

[50] C.B. Kalayci, A. Hancilar, A. Gungor, S.M. Gupta, Multi-objective fuzzy disassembly line balancing using a hybrid discrete artificial bee colony algorithm, J. Manuf. Syst. 37 (2015) 672–682.

[51] H. Liu, L. Zhang, Optimizing a disassembly sequence planning with success rates of disassembly operations via a variable neighborhood search algorithm, IEEE Access (2021).

[52] B. Yu, E. Wu, C. Chen, Y. Yang, B. Yao, Q. Lin, A general approach to optimize disassembly sequence planning based on disassembly network: A case study from automotive industry, Adv. Prod. Eng. Manag. 12 (4) (2017) 305–320.

[53] Z. Zhou, J. Liu, D.T. Pham, W. Xu, F.J. Ramirez, C. Ji, Q. Liu, Disassembly sequence planning: Recent developments and future trends, Proc. Inst. Mech. Eng. B 233 (5) (2019) 1450–1471.

[54] W.H. Chen, G. Foo, S. Kara, M. Pagnucco, Automated generation and execution of disassembly actions, Robot. Comput.-Integr. Manuf. 68 (2021) 102056.

[55] K. Li, Q. Liu, W. Xu, J. Liu, Z. Zhou, H. Feng, Sequence planning considering human fatigue for human–robot collaboration in disassembly, Procedia CIRP 83 (2019) 95–104.

[56] C. Xu, H. Wei, X. Guo, S. Liu, L. Qi, Z. Zhao, Human–robot collaboration multi-objective disassembly line balancing subject to task failure via multi-objective artificial bee colony algorithm, IFAC-PapersOnLine 53 (5) (2020) 1–6.

[57] G. Tian, Y. Ren, Y. Feng, M. Zhou, H. Zhang, J. Tan, Modeling and planning for dual-objective selective disassembly using AND/OR graph and discrete artificial bee colony, IEEE Trans. Ind. Inf. 15 (4) (2018) 2456–2468.

[58] Y. Ren, H. Jin, F. Zhao, T. Qu, L. Meng, C. Zhang, B. Zhang, G. Wang, J.W. Sutherland, A multiobjective disassembly planning for value recovery and energy conservation from end-of-life products, IEEE Trans. Autom. Sci. Eng. 18 (2) (2020) 791–803.

[59] T. Yin, Z. Zhang, Y. Zhang, T. Wu, W. Liang, Mixed-integer programming model and hybrid driving algorithm for multi-product partial disassembly line balancing problem with multi-robot workstations, Robot. Comput.-Integr. Manuf. 73 (2022) 102251.

[60] K. Wang, L. Gao, X. Li, P. Li, Energy-efficient robotic parallel disassembly sequence planning for end-of-life products, IEEE Trans. Autom. Sci. Eng. (2021).

[61] W. Xu, Q. Tang, J. Liu, Z. Liu, Z. Zhou, D.T. Pham, Disassembly sequence planning using discrete bees algorithm for human–robot collaboration in remanufacturing, Robot. Comput.-Integr. Manuf. 62 (2020) 101860.

[62] J. Liu, Z. Zhou, D.T. Pham, W. Xu, C. Ji, Q. Liu, Collaborative optimization of robotic disassembly sequence planning and robotic disassembly line balancing problem using improved discrete bees algorithm in remanufacturing, Robot. Comput.-Integr. Manuf. 61 (2020) 101829.
[63] W. Fang, W. Fan, W. Ji, L. Han, S. Xu, L. Zheng, L. Wang, Distributed cognition based localization for AR-aided collaborative assembly in industrial environments, Robot. Comput.-Integr. Manuf. 75 (2022) 102292.
[64] J. Pineau, M. Montemerlo, M. Pollack, N. Roy, S. Thrun, Towards robotic assistants in nursing homes: Challenges and results, Robot. Auton. Syst. 42 (3–4) (2003) 271–281.
[65] W. Bluethmann, R. Ambrose, M. Diftler, S. Askew, E. Huber, M. Goza, F. Rehnmark, C. Lovchik, D. Magruder, Robonaut: A robot designed to work with humans in space, Auton. Robots 14 (2) (2003) 179–197.
[66] R.R. Murphy, D. Riddle, E. Rasmussen, Robot-assisted medical reachback: a survey of how medical personnel expect to interact with rescue robots, in: RO-MAN 2004. 13th IEEE International Workshop on Robot and Human Interactive Communication (IEEE Catalog No. 04TH8759), IEEE, 2004, pp. 301–306.
[67] P. Tsarouchi, A.-S. Matthaiakis, S. Makris, G. Chryssolouris, On a human–robot collaboration in an assembly cell, Int. J. Comput. Integr. Manuf. 30 (6) (2017) 580–589.
[68] F. Ranz, V. Hummel, W. Sihn, Capability-based task allocation in human–robot collaboration, Procedia Manuf. 9 (2017) 182–189.
[69] M. Gombolay, A. Bair, C. Huang, J. Shah, Computational design of mixed-initiative human–robot teaming that considers human factors: situational awareness, workload, and workflow preferences, Int. J. Robot. Res. 36 (5–7) (2017) 597–617.
[70] A. Rosenfeld, A. Noa, O. Maksimov, S. Kraus, Human-multi-robot team collaboration for efficent warehouse operation, Auton. Robots Multirobot Syst. (ARMS) (2016).
[71] Q. Liu, Z. Liu, W. Xu, Q. Tang, Z. Zhou, D.T. Pham, Human–robot collaboration in disassembly for sustainable manufacturing, Int. J. Prod. Res. 57 (12) (2019) 4027–4044.
[72] I. Chatzikonstantinou, D. Giakoumis, D. Tzovaras, A new shopfloor orchestration approach for collaborative human–robot device disassembly, in: 2019 IEEE SmartWorld, Ubiquitous Intelligence & Computing, Advanced & Trusted Computing, Scalable Computing & Communications, Cloud & Big Data Computing, Internet of People and Smart City Innovation, IEEE, 2019, pp. 225–230.
[73] J. Huang, D.T. Pham, R. Li, M. Qu, Y. Wang, M. Kerin, S. Su, C. Ji, O. Mahomed, R. Khalil, et al., An experimental human–robot collaborative disassembly cell, Comput. Ind. Eng. 155 (2021) 107189.
[74] S. Parsa, M. Saadat, Human–robot collaboration disassembly planning for end-of-life product disassembly process, Robot. Comput.-Integr. Manuf. 71 (2021) 102170.
[75] M.-L. Lee, S. Behdad, X. Liang, M. Zheng, A real-time receding horizon sequence planner for disassembly in a human–robot collaboration setting, in: 2020 International Symposium on Flexible Automation, American Society of Mechanical Engineers Digital Collection, 2020, V001T04A004.
[76] M.-L. Lee, S. Behdad, X. Liang, M. Zheng, Disassembly sequence planning considering human–robot collaboration, in: 2020 American Control Conference, ACC, IEEE, 2020, pp. 2438–2443.
[77] M. Askarpour, D. Mandrioli, M. Rossi, F. Vicentini, Formal model of human erroneous behavior for safety analysis in collaborative robotics, Robot. Comput.-Integr. Manuf. 57 (2019) 465–476.
[78] I.G. Optimization, et al., Gurobi optimizer reference manual, 2021, URL http://www.gurobi.com.
[79] S.O. Sajedi, X. Liang, Uncertainty-assisted deep vision structural health monitoring, Comput.-Aided Civ. Infrastruct. Eng. 36 (2) (2021) 126–142.
[80] X. Liang, Image-based post-disaster inspection of reinforced concrete bridge systems using deep learning with Bayesian optimization, Comput.-Aided Civ. Infrastruct. Eng. 34 (5) (2019) 415–430.
[81] S. Hu, X. Zhang, H.-y. Liao, X. Liang, M. Zheng, S. Behdad, Deep learning and machine learning techniques to classify electrical and electronic equipment, in: International Design Engineering Technical Conferences and Computers and Information in Engineering Conference, American Society of Mechanical Engineers, 2021, V005T05A029.